Performance-based assessment of coupled bridge-ground systems

K.R. Mackie
University of Central Florida, Orlando, USA

J. Lu & A. Elgamal
University of California, San Diego, USA

SUMMARY:
Seismic risk assessment of urban transportation networks requires knowledge of bridge functionality and damage during earthquake events, often described using fragility or structure-specific hazard curves. Nonlinear time history analysis and consideration of coupled soil-foundation-structure effects may not be warranted for the design of individual highway overpass bridges. However, assessment of an inventory of bridges is unreliable using generic class fragilities due the variability in structural configurations, site conditions, and hazard. This paper demonstrates the effect of changing local site conditions (including potentially weak soil layers at some sites) on the response of a common reinforced concrete highway overpass structure. Response is quantified probabilistically in terms of post-earthquake repair costs and times and presented in terms of repair cost hazard contours maps. Similar in format to ground motion hazard maps, these contain additional structure-specific hazard information and allow rapid assessment of spatially-varying systems during a major event.

Keywords: fragility, weak soil, hazard, repair cost, loss modelling

1. INTRODUCTION

Seismic risk assessment of urban transportation networks requires knowledge of bridge functionality and damage during earthquake events, often described using fragility or structure-specific hazard curves. Nonlinear analysis under strong ground motion and consideration of coupled soil-foundation-structure effects may not be warranted for the design of individual highway overpass bridges. However, assessment of an inventory of bridges in a network is unreliable using generic class fragilities due the variability in structural configurations, site conditions, and hazard. Therefore, the development of enabling technologies that allow performance-based assessment is required. These technologies should allow performance assessment in terms of structural response, damage, or in terms of post-earthquake repair in a rapid fashion for a large suite of bridges and sites. The problem is not tractable if each scenario requires detailed knowledge in ground motion hazard, structural modeling, soil modeling, component and system-level damage assessment, and post-earthquake consequences.

This paper demonstrates the effect of changing local site conditions on the response of a common reinforced concrete highway overpass structure from the west coast of the USA (California). Two ground scenarios are developed: 1) a stiff soil site representative of good soil conditions not likely to experience liquefaction or require ground improvement, and 2) a site with weak upper soil strata that is likely to accumulate lateral and vertical deformations during excitation. Response is quantified probabilistically in terms of post-earthquake repair costs and times. BridgePBEE (http://peer.berkeley.edu/bridgepbee/), a graphical environment developed as an enabling performance-based assessment technology, was used to perform the computations. BridgePBEE couples a nonlinear dynamic analysis engine for bridge-ground systems with a performance-based earthquake engineering (PBEE) framework. This integration of hazard, modeling, analysis, and damage quantification allowed the generation of probabilistic repair models conditioned on earthquake

intensity for different soil classes in this paper. The results were computed in terms of repair cost and repair time hazard contour maps; however, only repair cost results are presented in this paper. The contour maps are similar in format to the ground motion hazard maps commonly employed in design, but contain additional structure-specific hazard information and allow rapid assessment of spatially-varying systems during a major event. In addition, such loss hazard maps can be used for design screening purposes. They effectively allow a single bridge-ground realization to be "moved" virtually around a stakeholder region, and the subsequent effect of the local ground motion hazard on the vulnerability of the structure is reflected in the loss hazard. Results show that different soil conditions can have a large impact on the performance of simple overpass bridges when evaluated in terms of repair cost (instead of only permanent deformations, for example), and that the results can be readily extended to entire regions defined in terms of existing ground motion hazard data.

The basis for developing BridgePBEE was rooted in ongoing developments in the performance-based earthquake engineering (PBEE) community. Beyond traditional geotechnical and structural response metrics, PBEE aims to quantify the seismic performance and risk of engineered facilities using metrics that are of immediate use to both engineers and stakeholders. PBEE as applied to buildings has seen rapid development and adoption recently (e.g., ATC-58 and ATC-63); however, in the bridge and infrastructure arena, there have been relatively few attempts (Solberg et al., 2008; Mackie et al., 2008; Bradley et al., 2010) at rigorous development of the data necessary for PBEE or packaging the tools in a form that allows rapid PBEE-based evaluation and assessment such as PACT.

Mackie and co-workers pioneered the development of a bridge performance-based analysis framework (Mackie et al., 2008; Mackie et al., 2010). Bridges with fixed or spring foundation constraints were studied within this framework using the Pacific Earthquake Engineering Research (PEER) center's computational platform OpenSees (http://opensees.berkeley.edu/). Based on the response of a series of typical pre-stressed, single-column bent, multi-span, box girder bridges in California, the data flows and requisite information were derived to relate response to damage of individual components within the structure, denoted as performance groups (PGs). Damage to these PGs were tied to explicit repair procedures and repair quantities that could then be used for cost estimation and repair effort necessary to return the bridge to its original level of functionality (direct costs). The data flows and framework are extensible to other bridge classes; however, to date only repair, cost, and schedule data have been obtained for the typical reinforced concrete box girder overpass bridges used in the pilot studies.

Simultaneously, Elgamal and co-workers (Lu et al., 2006; Elgamal and Lu, 2009) had embarked on development of a three-dimensional (3D) ground-foundation graphical user interface OpenSeesPL that employs OpenSees as the finite element (FE) analysis engine. This interface allows for the execution of pushover and seismic single-pile or pile-group ground simulations. OpenSeesPL includes pre- and post-processing capabilities to generate the mesh, define material properties and boundary conditions, activate OpenSees to conduct the computations, and display/animate the output responses (http://cyclic.ucsd.edu/openseespl/). Various ground modification scenario studies were enabled by appropriate specification of the material within the pile zone. The menu of soil materials in OpenSeesPL includes a complementary set of soil modeling parameters representing loose, medium and dense cohesionless soils (with silt, sand or gravel permeability), and soft, medium and stiff clay (J2 plasticity cyclic model).

BridgePBEE was the enabling software tool that integrated: i) an implementation of a PBEE framework within a graphical user-interface, ii) a module for handling the needed input ground motion ensemble and to compute all salient characteristics, denoted as intensity measures (IMs), iii) modify the graphical interface to automatically generate user-defined bridge-ground FE models, and iv) build the post-processing capability to display the seismic response ensembles, and to display the PBEE outcomes. BridgePBEE was used to generate the two bridge-ground scenarios used in this paper, as well as the loss hazard contour maps. A brief description of the underlying framework and bridge-ground models are presented in the next sections. More detailed information can be found in earlier publications on the development of BridgePBEE (Mackie et al., 2010). More information on the two soil scenarios considered in this paper (as well as an additional set of two soil scenarios not presented

here) can be found in Mackie et al. (2012).

2. PBEE FRAMEWORK AND BRIDGEPBEE ELEMENTS

PBEE considers seismic hazard, structural response, resulting damage, and repair costs associated with restoring a structure to its original function, using a fully consistent, probabilistic analysis of the associated parts of the problem (Cornell and Krawinkler, 2000). The uncertainty surrounding the PBEE framework components necessitates a probabilistic approach and acceptance criteria based on levels of confidence that probabilities of failure are acceptably small. Adoption of such PBEE methodology in practice requires abandonment of prescriptive seismic safety specifications and acceptance of performance objectives defined in terms of quantities familiar to engineers, owners, managers, and stakeholders alike. A rigorous yet practical implementation of the PEER PBEE methodology was adapted for use in BridgePBEE. The methodology is subdivided to achieve performance objectives stated in terms of the probability of exceeding threshold values, or annual rates of exceedance, of socio-economic decision variables (DVs) in the seismic hazard environment under consideration. The PEER PBEE framework utilizes the total probability theorem to disaggregate the problem into several intermediate probabilistic models. This disaggregation of the decision-making framework outcome involves the following intermediate variables: repair quantities (Q), damage measures (DMs), engineering demand parameters (EDPs), and seismic hazard intensity measures (IMs). Consequently, engineers may choose to scrutinize probabilities of exceeding an EDP, such as strain, while an owner may choose to scrutinize probabilities of exceeding a DV, such as repair cost.

An important step enabling effective aggregation of decision data was the association of structural elements and assemblies into performance groups (PGs) based on commonly used repair methods. The numerical implementation of the methodology is described in Mackie et al. (2010). The major components of a PBEE analysis are: specification of ground motions, mesh and soil constitutive model determination, bridge superstructure model and constitutive model determination, specification of PGs and the associated PBEE quantities, and post-processing of the results. During transient analysis for each ground motion, response quantities are tracked at each time step. The response quantities of interest are tied directly the PGs that are used in the PBEE analysis for assessing damage and repair. Each PG contains a collection of components that reflect global-level indicators of structural performance and that contribute significantly to repair-level decisions. The notion of a PG allows grouping several components for related repair work; therefore PGs are not necessarily the same as the individual load-resisting structural components.

The PGs (and associated EDP) used in the bridges presented in this paper are: PG1 - maximum column drift ratio, PG2 - residual column drift ratio, PG3 - maximum relative left deck-end/abutment displacement, PG4 - maximum relative right deck-end/abutment displacement, PG5 - maximum absolute bearing displacement (left abutment), PG6 - maximum absolute bearing displacement (right abutment), PG7 - approach residual vertical displacement (left abutment), PG8 - approach residual vertical displacement (right abutment), PG9 – left abutment residual pile cap displacement, PG10 – right abutment residual pile cap displacement, and PG11 - column residual pile cap displacement. This selection of PGs is a subset of the initial PGs used in Mackie et al. (2008) due to the consideration of an overpass bridge with only a single bent.

Discrete damage states (DS) are defined for each performance group. Each damage state has an associated repair method that also has a subset of different repair quantities (Qs). Once the Qs have been established for a given scenario (damage to different PGs), the total repair costs can be generated through a unit cost function. In addition, an estimate of the repair effort can be obtained through a production rate for each Q. The user has the ability to modify the default values specified for all of the repair quantities per damage state, unit costs, and production rates. More information on the derivation of the default DSs, Qs, unit costs, and production rates can be found in Mackie et al. (2008) and Mackie et al. (2011). For the purposes of the user interface, an estimate of the replacement cost of the bridge is automatically generated based on the square footage of the deck and the Caltrans

Comparative Bridge Costs (CBC) data, corrected to be consistent with the year 2007 cost data used in the calibration of the unit costs. The CBC includes a 10% mobilization cost but does not include any costs for demolition or removal of existing infrastructure.

To facilitate computation time, individual transient analyses can be run in parallel on a multi-processor machine. However, once the response quantities have been computed, PBEE scenarios can be independently investigated without re-running the model. Computation time for the PBEE analysis is negligible; hence it was easy to repeat for different hazard scenario locations in this paper. All motions were obtained from the PEER NGA database (http://peer.berkeley.edu/nga/). An ensemble of 100 selected ground motions was employed in the PBEE analysis illustrated in this paper. Each motion is composed of 3 perpendicular acceleration time history components (2 lateral and one vertical). These motions were selected through earlier efforts and were selected to be representative of seismicity in typical regions of California. The motions are divided into 5 bins of 20 motions each with characteristics: i) moment magnitude (Mw) 6.5-7.2 and closest distance (R) 15-30 km, ii) Mw 6.5-7.2 and R 30-60 km, iii) Mw 5.8-6.5 and R 15-30 km, iv) Mw 5.8-6.5 and R 30-60 km, and v) Mw 5.8-7.2 and R 0-15 km. For the results presented in this paper, only peak ground velocity (PGV) is used as an IM. Ground motion hazard data was obtained from USGS continental USA hazard data for peak ground acceleration (PGA) gridded by latitude and longitude (USGS, 2008). Each of the three probabilities of exceedance in 50 years (2%, 5%, and 10%) were used to fit a power-law relationship between the mean annual frequency of exceedance and the intensity.

To be consistent with the PBEE results (and previous probabilistic seismic demand models generated for the bridges), the hazard was converted from PGA to PGV using a conversion factor of 36 in/sec/g. Ideally, the hazard for PGV would be obtained directly or converted from PGA using site-specific ground profile information. However, for comparison purposes in this paper, the same factor was used for all locations and both of the soil scenarios investigated (assuming the ground motions were base input motions). The 36 in/sec/g is based loosely on Mohraz (1975) for a site with less than 30 ft of alluvium underlain by rock (mean value using horizontal component with larger peak PGA as suggested), and was specifically selected to be lower than the standard 48 in/sec/g conversion used in Newmark spectra for firm ground. The resulting PGV (cm/s) hazard curves for California used in the loss hazard analysis are shown in Figure 2.1. The vertical and horizontal axes show latitude and longitude in units of degrees north and west, respectively (actually the negative of the longitude is shown).
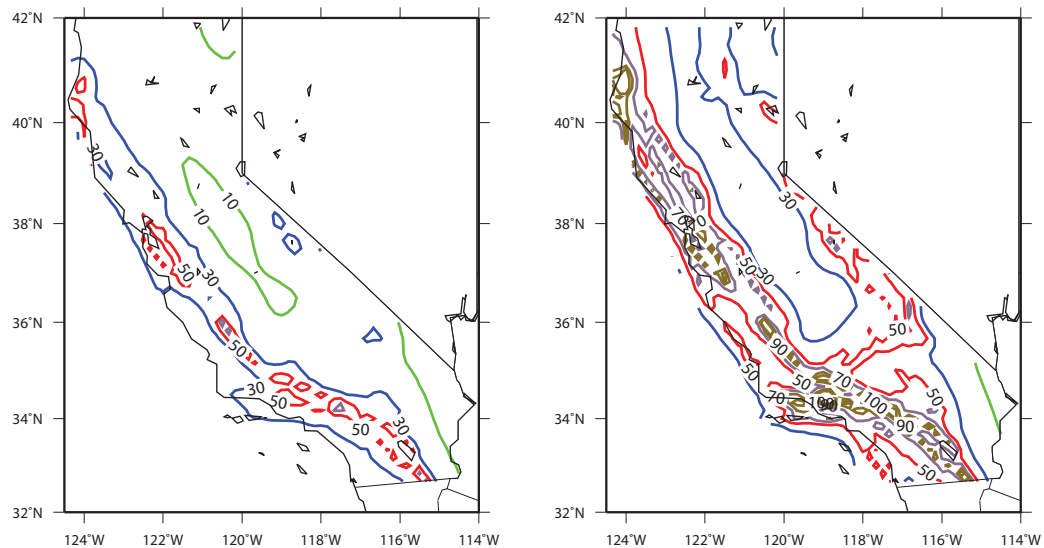
Figure 2.1. Ground motion hazard maps for California showing PGV (cm/s) at 10% (left) and 2% (right) probabilities of exceedance in 50 years.

3. BRIDGE AND SOIL PROFILES

The bridge-ground configurations are all based on single column bent, box girder, reinforced concrete bridges. This class of structures is intended to be typical of bridges in California that are designed according to the Caltrans Seismic Design Criteria and can be classified as Ordinary Standard Bridges (OSBs). OSBs are those with lengths less than 91.4 m, standard abutment and bent cap details, and standard foundations on soil that do not require extensive site work. The bridge dimensions considered in this paper are 45.7 m spans, 6.71 m clear column heights, 1.22 m circular column diameter, 11.9 m wide two-cell box girder, and seat-type abutments. The properties were derived from the Type 1 class of bridge designs presented in Ketchum et al. (2004). The soil domain is 441 m long, 441 m wide and 30 m deep. The complete bridge-foundation-ground mesh is shown in Figure 3.1. Mesh refinement was performed to create elements with the smallest aspect ratio near the foundations of the bridge (pile and embankments).
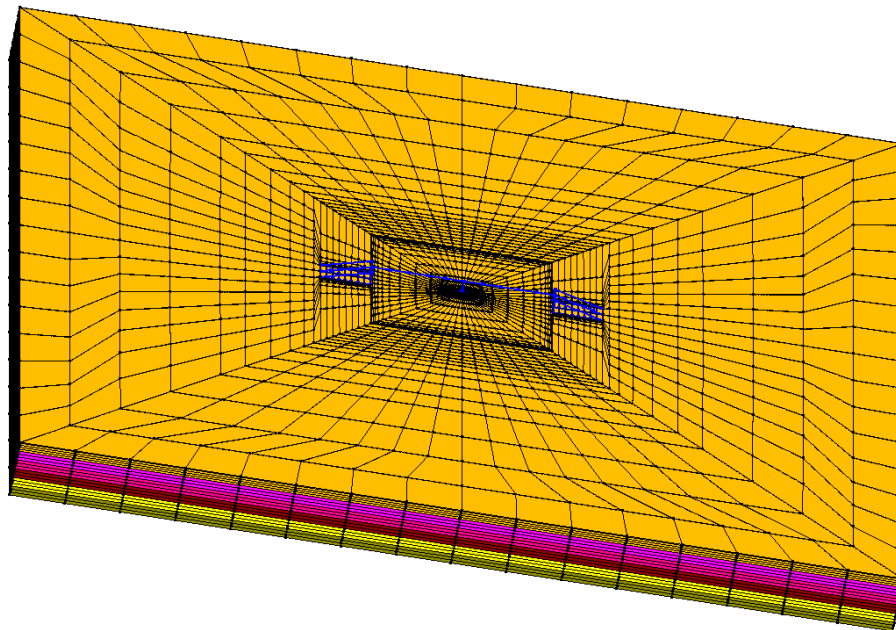
Figure 3.1. Finite element domain showing soil extents and bridge/approach mesh in the center. Mesh refinement was performed surrounding the center bent pile as well as the approaches.

The columns are modeled as nonlinear beam-column elements with fiber cross sections. The deck is also modeled using two-noded beam-column elements discretized into five separate elements along each clear span. The deck is assumed to be capacity designed so that it responds in the elastic range, with cracked section properties specified for this bridge. Detailed modeling considerations and constitutive model properties of the superstructure elements can be found in Mackie et al. (2008). The approach ramp model connects the bridge longitudinal boundaries to the ground using a trapezoidal arrangement of rigid link elements that extends 0.5 m into the soil domain below the abutments. The rigid link assembly captures the embankment and approach geometry and permits interaction with the bridge at its ends, including the potential embankment settlement into the surrounding soil (Elgamal et al., 2008).

An abutment model provides the interface between the approach ramps and the bridge ends. The spring abutment model was used to better simulate the seat-type abutment in the bridge configuration studies in this paper. The spring abutment model includes longitudinal, transverse, and vertical nonlinear behavior (Aviram et al., 2008). Longitudinal response is based on the system response of the elastomeric bearing pads, gap, abutment back wall, abutment piles, and soil backfill material. Prior to

gap closure, the superstructure forces are transmitted through the elastomeric bearing pads to the stem wall, and subsequently to the piles and backfill, in a series system. After gap closure, the superstructure bears directly on the abutment back wall and begins to mobilize the passive backfill pressure. A system of zero-length elements is distributed along two rigid elements oriented in the transverse bridge direction, connected together by bearing pads. Transverse response is based on the system response of the elastomeric bearing pads, exterior concrete shear keys, abutment piles, wing walls, and backfill material. The transverse stiffness and strength of the backfill, wing wall, and pile system is calculated using a modification factor on the longitudinal properties. Stiffness and strength are distributed equally to the two extreme zero-length elements of the second rigid element. Vertical response of the abutment model includes the vertical stiffness of the bearing pads in series with the vertical stiffness of the trapezoidal embankment. The abutment is assumed to have a nominal mass proportional to the superstructure dead load at the abutment, including a contribution from structural concrete. Model details are provided in Aviram et al. (2008).

In the original Ketchum et al. (2004) foundation, the column bent was founded on a 0.91 m diameter cast-in-drilled-hole (CIDH) 2x2 pile group. However, to reduce the finite element soil mesh complexity around the foundation, a single pile shaft was introduced. For simplicity, the cross section and reinforcement of the pile shaft was assumed to be continuous with the column above and below grade, as with a Type I Caltrans pile shaft. Therefore, the same nonlinear fiber cross sections were used with displacement-based beam-column elements. The shaft diameter was represented by lateral rigid links with outer node displacement degrees of freedom constrained with adjacent soil mesh nodes (Elgamal et al., 2008) along the 20 m height of the pile shaft.

Near the ground surface, soil response to seismic excitation is assumed to be predominantly caused by vertically propagating shear waves. Thus, in the free field (away from the bridge), the lateral response of the soil domain is expected to closely match that of a conventional shear beam. In this regard, the longitudinal/transverse mesh lateral boundaries with idealized identical soil profiles are constrained to undergo the same vertical and longitudinal/transversal motions (at any given depth) using multi-point constraints in OpenSees. These lateral boundaries are located as far as possible from the bridge so as to decrease any effect of these boundary conditions on the bridge response (Elgamal et al., 2008). The same soil domain geometry (depth, boundary conditions, and extents) is used for all scenarios, which are delineated by different material properties and layer definitions. The typical (California) soil profile used for cast-in-drilled-hole piles (CIDH) and pipe piles in Ketchum et al. (2004) was used as a template for the stiffness and strength properties by soil strata that define Scenario 1. From this typical profile, a variation was derived to highlight the potential influence of the ground layers in terms of relative flexibility of the soil around the pile, and susceptibility to the accumulation of permanent deformations, denoted as Scenario 2.

Bridge-Ground Scenario #1: Stiff Soil Profile

The FE model includes 20,181 nodes and 18,800 nonlinear solid brick elements (bbarBrick). A benchmark soil profile was generated that includes cohesive soil strata with gradually increasing shear moduli and undrained shear strengths, more details of which can be found in Mackie et al. (2012). The OpenSees constitutive model used for all layers is PressureIndependentMultiYield, with parameters of the constitutive model determined from the soil properties by shear wave velocity, cohesion, mass density, and bulk modulus (all layers were assumed to have a Poisson's ratio of 0.45). In this hysteretic multi-yield surface pressure-independent (von Mises) idealization, a hyperbolic backbone curve defines the nonlinear shear response with peak shear strength Su reached at 3% octahedral shear strain. The soil profile is idealized into six sublayers (each sublayer is 5 m thick). The ground water table in the original profile was at 2.4 m, but does not affect the pressure independent materials selected in the analysis.

Bridge-Ground Scenario #2: Shallow Soft Ground Stratum

In Scenario 2, the upper 3 layers are replaced with weaker strata. This configuration provides support

for the column at depth, while allowing significant seismically induced deformations (both laterally and vertically) to potentially accumulate within the shallow layers. In addition, at higher acceleration levels, the upper strata have the propensity for reduced peak ground surface accelerations as the shear strength attained decreases. A series of sensitivity studies was performed to determine the properties of the top three soil layers that cause realistic settlement and lateral deformation. The properties were selected to create potential permanent lateral deformation at the center bent foundation that would consequently mobilize foundation repairs in the PBEE analysis. In addition, permanent settlement at the abutments was targeted to allow the introduction of embankment and abutment actions.

4. RESULTS

The different soil profiles have a significant effect on the level of ground shaking experienced at the base of the bridge structure. The weak soil case (Scenario 2) provides an isolation effect that prevents the same level of accelerations being transmitted to the column, and thereby actually reduces some of the costs associated with column repairs (as compared to the stiffer soil scenario). In addition, lateral spreading occurs during many ground motions, and the reduced shear strength results in a considerable vertical settlement after shaking. Figure 4.1 shows the longitudinal elevation deformed mesh at the end of strong shaking for the SCS (Sylmar converter station) motion. Due to the lack of deep piles (such as those below the column), the vertical settlement at both abutments reaches 0.5 m. The noticeable feature of the mesh is that settlement at the abutment pulls down the deck through the abutment connection to the superstructure (elastomeric bearings with dowels), which is not well captured by the repair methods employed in the PBEE framework. However, in addition to the vertical settlement, there is lateral movement, particularly between the top of the back wall and the abutment foundation because of the axial rigidity of the deck. This lateral movement causes significant lateral movement at the abutment connection, and does result in significant damage and repair to the bridge.
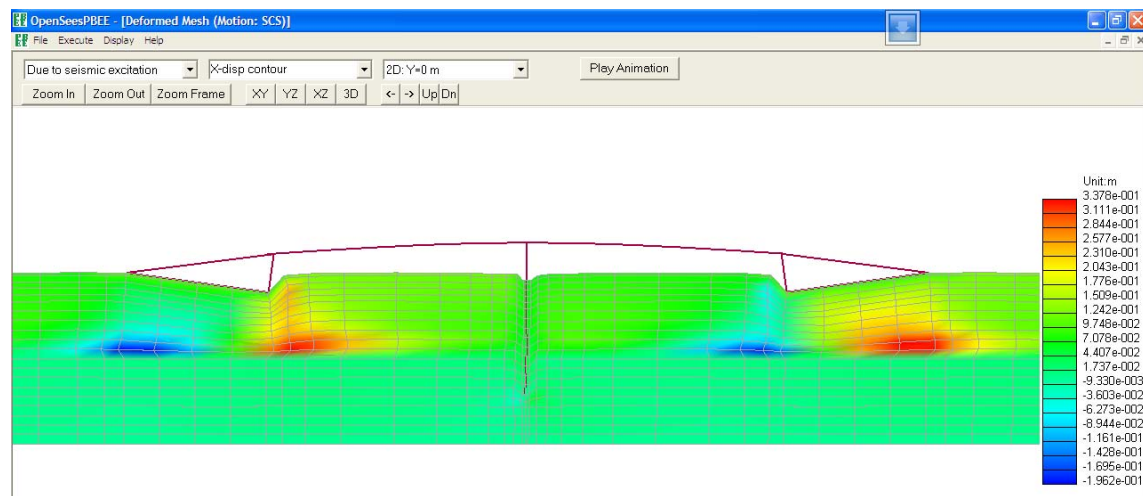
Figure 4.1. Bridge-ground scenario 2 (weak soil) deformed mesh (2D longitudinal cross section) for SCS motion at 45.0139 sec.

Complete PBEE computations were performed to obtain intensity-dependent repair cost ratios (RCRs) and repair times (RTs), although only RCR results are presented here for sake of brevity. For the figures presented in the paper, only the base input PGV is used as the IM (SRSS of both lateral components). However, it should be noted that the attenuation of the motion through the soil profiles causes significantly different excitation at the free-field level. Therefore, similar loss curves can be generated using the free-field PGV; however, they illustrate the same trends as the input PGV, so are not included here. For all scenarios, the consequences of shaking and repair do not begin to accumulate until a PGV of approximately 20 cm/s. The weak soil case results in the largest RCR for intensities between 20 and 60 cm/s. However, numerous other interesting conclusions can be drawn as

the intensities increase. For example, the stiff soil scenario accumulates the least cost (as would be expected) in addition to reaching a plateau above which the cost does not continue to increase. This is representative of the fact that the foundation PGs do not contribute to the repair and the intensities are not sufficient to cause failure and complete column replacement. Finally, the weak soil case also exhibits a cost plateau, but continues to increase rapidly with intensity beyond this due to the accumulation of damage to the foundations that result in RCRs that approach the replacement cost of the bridge.

The RCR loss models derived for each scenario were convolved with the ground motion hazard curves presented previously (actually with the power-law fit to the three discrete hazard levels). The procedure was repeated for a multitude of grid points within the state of California to generate the RCR loss hazard curves. The two levels presented correspond to the 1% and 2% probabilities of exceedance in 75 years. The change to a 75-year return period was executed to be consistent with hazard characterization in AASHTO. The hazard curves corresponding to Scenario 1 (stiff soil) are shown in Figure 4.2 and the hazard curves corresponding to Scenario 2 (weak soil) are shown in Figure 4.3. The 2%-in-75-year probability of exceedance contours peak at 40% RCR and 70% RCR for Scenario 1 and Scenario 2, respectively. The 1%-in-75-year probability of exceedance contours peak at 50% RCR and 80% RCR for Scenario 1 and Scenario 2, respectively.
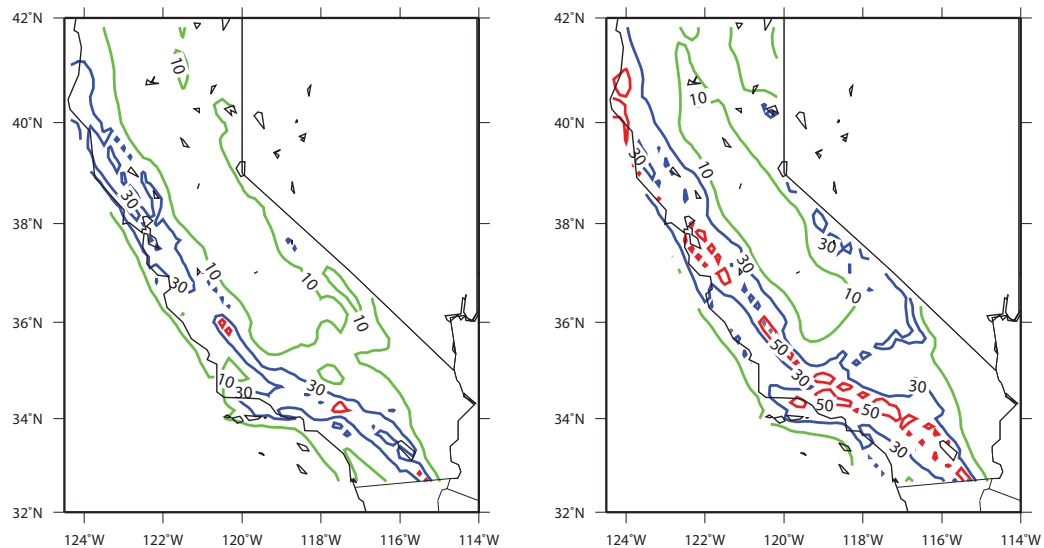
Figure 4.2. Bridge-ground Scenario 1 (stiff soil) repair cost ratio (in %) loss hazard curve with 2% (left) and 1% (right) probabilities of exceedance in 75 years.

Clearly, there is a relationship between regions delineated with high loss hazard curves and those with high ground motion hazard contours; however, the loss hazard curves are significantly richer in information content. The intensity-dependent loss models generated by BridgePBEE reflect different repair methods and actions as the ground motion intensity varies. In addition, the rate of accumulation of repair quantities is dependent on the intensity. Therefore, in regions dominated by close distance, high magnitude, events, the RCR distribution will be markedly different than regions where hazard has more uniform contributions from different magnitudes and distances, for example. The ranges of intensity where repair costs do not continue to increase until a more serious repair action is necessary lead to a smoothing of ground motion hazard contours.
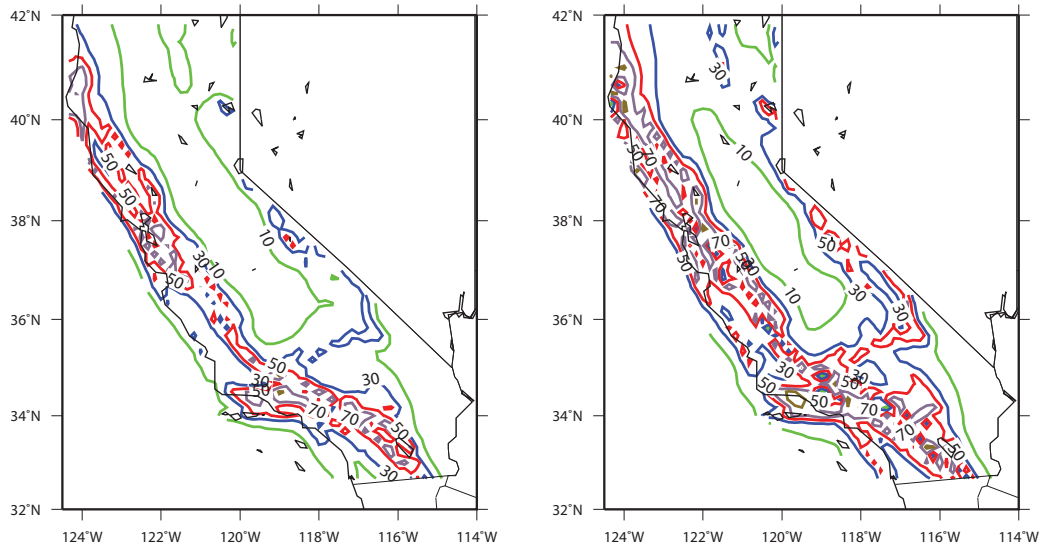
Figure 4.3. Bridge-ground Scenario 2 (weak soil) repair cost ratio (in %) loss hazard curve with 2% (left) and 1% (right) probabilities of exceedance in 75 years.

The contours allow a direct comparison of how vulnerable the given bridge design would be when moved to different potential locations within the region, as well as how the vulnerability would change with weaker upper soil layers at individual sites. From the two soil scenarios presented in this paper, it can be seen that ignoring the ground component in an analysis, and the corresponding bridge-ground interaction, can be misleading. For example, comparisons of Figures 4.2 and 4.3 reveal that RCRs may shift by more than 40% (Scenario 2 being higher) in certain regions. As discussed, these increases in predicted RCR hazard are not uniform for all locations in the region due to the different repair actions triggered according to the contributions coming from the ground motion hazard.

5. DISCUSSION AND CONCLUSIONS

Performance-based evaluations of bridge systems in past research were limited to superstructure-only models, or may have included rudimentary representations of foundations; however were then coupled with performance assessments that did not address post-earthquake consequences expressed in economic terms. Combining high fidelity coupled bridge-foundation-ground numerical models with a PBEE framework in a graphical user environment has enabled such studies to be more readily accessible. The BridgePBEE environment was utilized in this paper to investigate the variation in repair costs for a two-span ordinary standard bridge founded on two different soil scenarios. Definition of the bridge-ground configuration, material properties, ground motion selection, and PBEE performance group and repair parameters is greatly facilitated, enabling evaluation of multiple ground motions, and multiple ground motion hazard locations.

Scenario 2 (the weaker upper soil strata) results in the largest post-earthquake repairs; however, the increases are not uniform across all PGs as the poor soil layers act as a form of isolation, preventing larger forces from entering and damaging the superstructure. The intensity-dependent disaggregation of repairs by repair quantity or PG show that the engagement of repair actions at different intensities. Foundation and abutment repairs are dominant at the 2%-in-50 year exceedance probability hazard level. The more frequent events (the 50%-in-50 year level for example), repairs such as bearing replacement and superficial concrete patching or epoxy injection become more common. Therefore, the convolution of the intensity-dependent repair cost models with ground motion hazard data results in more information rich loss hazard curves.

While some detail is lost in the figures presenting repair cost ratio (RCR) hazard over the entire state of California for the two bridge-ground scenarios, the additional information allows for quick design screening as well as rapid assessment after a large event. Resources can be targeted to locations with known consequence-based vulnerabilities rather than simply regions with higher ground motion hazards. Refinement of the contour maps to district or city levels also allows more detailed investigations of proposed bridge-ground systems, particularly if more information is known about the existing site profiles. Currently, the results presented in this paper are limited because it is assumed the same bridge-ground system can appear anywhere in the state, which is not consistent with soil maps that may be available for a region. In addition, it is assumed that the input ground motion hazard is also not dependent on the local site; therefore, the same PGA (or PGV conversion in this case) is used for all locations as an input to the base of the meshes.

REFERENCES

Aviram, A., Mackie, K.R. and Stojadinovic, B. (2008). Effect of abutment modeling on the seismic response of bridge structures. *Earthquake Engineering and Engineering Vibration* 7(4), 395-402.

Bradley, B.A., Cubrinovski, M., Dhakal, R.P. and MacRae, G.A. (2010). Probabilistic seismic performance and loss assessment of a bridge–foundation–soil system. *Soil Dynamics and Earthquake Engineering* 30, 395-411.

Cornell, C.A. and Krawinkler, H. (2000). Progress and challenges in seismic performance assessment. *PEER Center News* 3(2).

Elgamal, A. and Lu, J. (2009). A framework for 3D finite element analysis of lateral pile system response. *Geotechnical Special Publication No. 186*, International Foundations Congress and Equipment Expo'09, Orlando FL, pp. 616-623.

Elgamal, A., Yan, L., Yang, Z. and Conte, J.P. (2008). Three-dimensional seismic response of Humboldt Bay bridge-foundation-ground system. *Journal of Structural Engineering* 134(7), 1165-1176.

Ketchum, M., Chang, V. and Shantz, T. (2004). Influence of design ground motion level on highway bridge costs. *Report No. Lifelines 6D01*, Pacific Earthquake Engineering Research Center, Berkeley CA.

Lu, J., Yang, Z. and Elgamal, A. (2006). OpenSeesPL three-dimensional lateral pile-ground interaction version 1.00 user's manual. *Report No. SSRP-06/03*, Department of Structural Engineering, University of California, San Diego CA.

Mackie, K.R., Lu, J. and Elgamal, A. (2010). User interface for performance-based earthquake engineering: a single bent bridge pilot investigation. *9th US National and 10th Canadian Conference on Earthquake Engineering*, Toronto Canada.

Mackie, K.R., Lu, J. and Elgamal, A. (2012). Performance-based earthquake assessment of bridge systems including ground-foundation interaction. *Soil Dynamics and Earthquake Engineering*, under review.

Mackie, K.R., Wong, J-M. and Stojadinovic, B. (2008). Integrated probabilistic performance-based evaluation of benchmark reinforced concrete bridges. *Report No. 2007/09*, Pacific Earthquake Engineering Research Center, Berkeley CA.

Mackie, K.R., Wong, J-M. and Stojadinovic, B. (2010). Post-earthquake bridge repair cost and repair time estimation methodology. *Earthquake Engineering Structural Dynamics* 39(3), 281-301.

Mackie, K.R., Wong, J-M. and Stojadinovic, B. (2011). Bridge damage and loss scenarios calibrated by schematic design and cost estimation of repairs. *Earthquake Spectra* 27, 1127-1145.

Mohraz, B. (1975). A study of earthquake response spectra for different geological conditions. *Bulletin of the Seismological Society of America* 66(3), 915-935.

Solberg, K.M., Dhakal, R.P., Mander, J.B. and Bradley, B.A. (2008). Computational and rapid expected annual loss estimation methodologies for structures. *Earthquake Engineering and Structural Dynamics* 37, 81-101.

United States Geological Survey. (2008). *Earthquake hazards program,* http://earthquake.usgs.gov/research/hazmaps/